Electronic Supplementary Material (ESI) for Nanoscale.


## Supplemental Information for

Surface enhanced Raman scattering of extracellular vesicles from clinical cancer biofluids reveals lipoprotein contamination varies with isolation methodology

Hanna J. Koster[1], Tatu Rojalin[1], Alyssa Powell[1], Dina Pham[1], Rachel R. Mizenko[1], Andrew Birkeland[2], Randy P. Carney[1]

[1]Department of Biomedical Engineering, University of California, Davis, Davis, CA 95616, USA
[2]Department of Otolaryngology – Head and Neck Surgery, University of California, Davis, Sacramento, CA 95817, USA

**Supplementary Table 1**: **SERS peak assignments.** Chemical assignments for annotated peak regions in **Figures 4 – 8** in the main text, including literature references. When a specific peak of interest from our analysis was contained with a few (<5) inverse centimeters of a literature value, we replaced the specific value with a range rounded to the nearest value of "5" or "10" for ease of interpretation, given that our spectral resolution is within an error of 5 $cm^{-1}$.

| Wavenumber region ($cm^{-1}$) | Chemical assignment | Reference |
|---|---|---|
| 720 | Amino acids | [1] |
| 790-795 | Nucleic acids | [2,3] |
| 840-855 | Nucleic acids and e.g., ring deformation in tyrosine | [2] |
| 900 | Carbohydrate-related; proline/valine/glycogen | [4,5] |
| 926 | C-C ring stretching e.g., proline, nucleic acids | [2] |
| 1005-1010 | Symmetric ring breathing; phenylalanine | [1] |
| 1025 – 1050 | $CH_2CH_3$ bending, e.g., lipid | [1,6-8] |
| 1120 – 1190 | C-C, e.g., lipid; C-N amide in proteins | [1,6-9] |
| 1149 | Carotenoids | [8] |
| 1165 | Carbohydrate-related | [7] |
| 1235 | C-N stretching + N-H deformations; amide III proteins | [7] |
| 1265 – 1280 | Amide III protein and C=C fatty acid | [7,8] |
| 1282 | $CH_2$, $CH_3$ deformations; C-N stretching | [7] |
| 1320 – 1360 | $CH_2CH_3$ in nucleic acids | [7] |
| 1376 | $CH_3$ symmetric in lipid | [7] |
| 1405 – 1440 | CH rocking in lipid | [1] |
| 1450 – 1465 | $CH_2/CH_3$, lipid and protein | [9] |
| 1480 – 1485 | C-H, lipid and protein | [7] |
| 1495 – 1515 | Vibrations from C=C conjugations | [1] |
| 1520 – 1565 | Tryptophan | [7] |
| 1545 – 1590 | Amide II | [10,11] |
| 1603 | Cytosine and phenylalanine | [1] |
| 1620 | DAMP/C=C protein | [7] |
| 1630-1650 | Amide I, C=C | [9,10] |

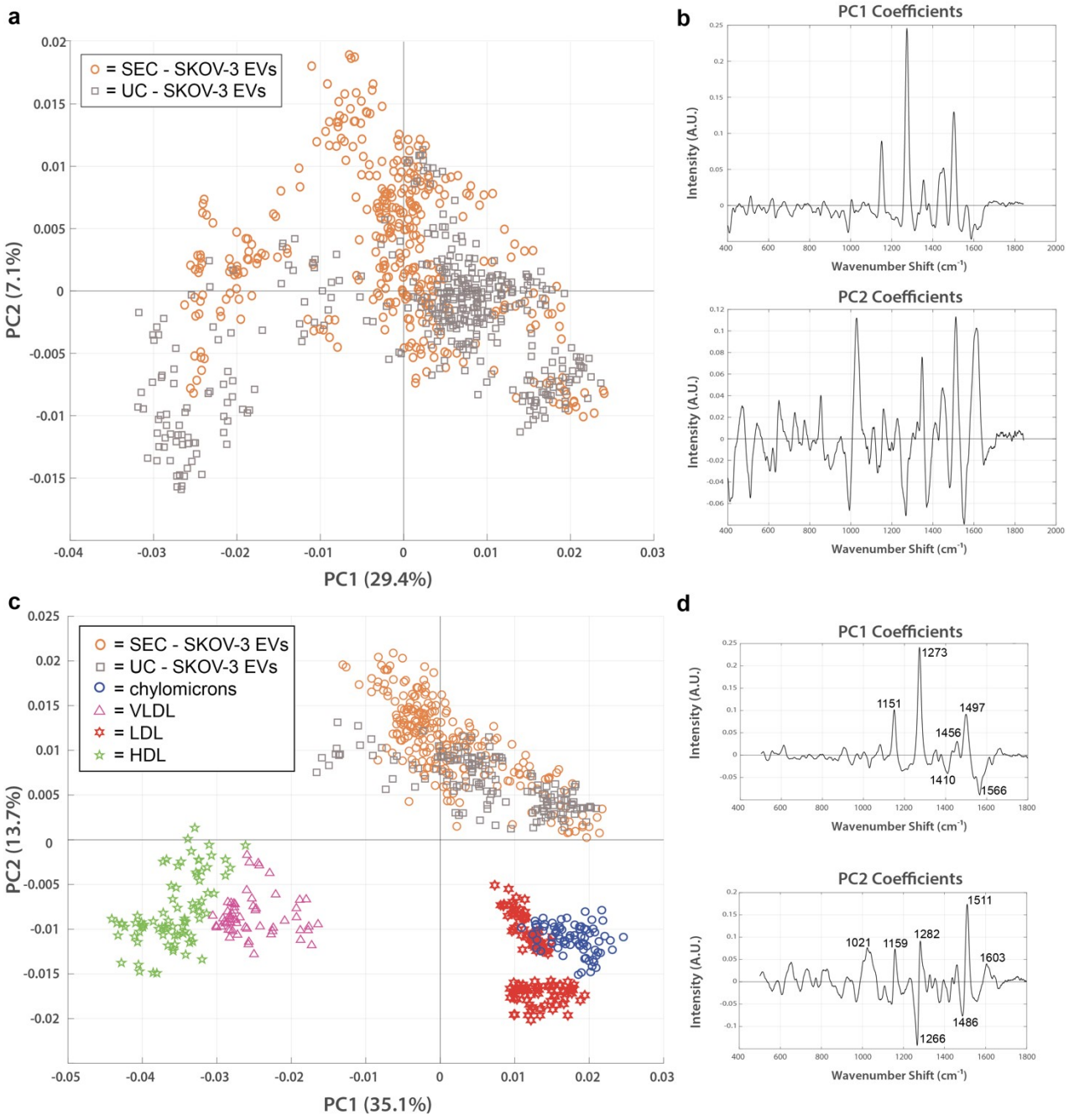


**Supplementary Figure 1: PCA analysis of EVs isolated from cell culture supernatant compared to lipoprotein standards. (a)** EVs isolated from SKOV-3 cell culture supernatant are chemically similar to each other regardless of which isolation method is used. EVs isolated by SEC (orange) and UC (gray) heavily overlap in PC space without clear separation along their major principal components. **(b)** PC1 and PC2 loadings represent the greatest amount of chemical variation between samples in panel (a). **(c)** When analyzed with the lipoprotein standards, there is clear separation between the EVs and lipoprotein subpopulations, indicating a lack of chemical overlap between the species. **(d)** PC1 and PC2 loadings for panel (c). The positive peaks driving this separation indicate carbon-carbon and carbon-nitrogen stretching and deformations in proteins and lipids (1021 $cm^{-1}$, 1159 $cm^{-1}$, 1282 $cm^{-1}$), as well as unsaturated fatty acids (1511 $cm^{-1}$).

**Supplementary Table 2: Quality performance metrics for EVs isolated by various methods and tested with various machine learning (ML) classifiers.** Each isolation method (DG, SEC, UC, or UC+SEC) was subjected to either QDA and LDA over the first two or three PCs. Accuracy, sensitivity, and specificity were calculated for each case, using the predicted class (cancer vs. non-cancer) from the SERS assay against the true class by clinical histopathological analysis. Bold black boxes highlight the top performing (i.e., most accurate) method for each isolation method. The boxes are shaded from green to red to represent the linear range from the highest metric (100%) to the lowest (82.7%).

| | | Algorithm (PCs included) | | | |
|---|---|---|---|---|---|
| Isolation method | | QDA (PC1-PC2) | QDA (PC1-PC3) | LDA (PC1-PC2) | LDA (PC1-PC3) |
| DG | Accuracy | **98.2** | **98.3** | **97.4** | **97.2** |
| | Sensitivity | 97.8 | 98.3 | 95.7 | 95.3 |
| | Specificity | 98.9 | 98.4 | 100.0 | 100.0 |
| SEC | Accuracy | **96.3** | **96.7** | **97.8** | **97.8** |
| | Sensitivity | 95.4 | 95.4 | 96.0 | 96.0 |
| | Specificity | 97.2 | 98.0 | 99.8 | 99.8 |
| UC | Accuracy | **98.0** | **98.0** | **96.0** | **96.9** |
| | Sensitivity | 97.1 | 97.1 | 92.5 | 94.4 |
| | Specificity | 99.0 | 99.0 | 99.6 | 99.4 |
| UC+SEC | Accuracy | **85.8** | **86.5** | **85.8** | **86.0** |
| | Sensitivity | 84.7 | 82.7 | 84.6 | 85.4 |
| | Specificity | 87.4 | 92.2 | 87.7 | 86.9 |

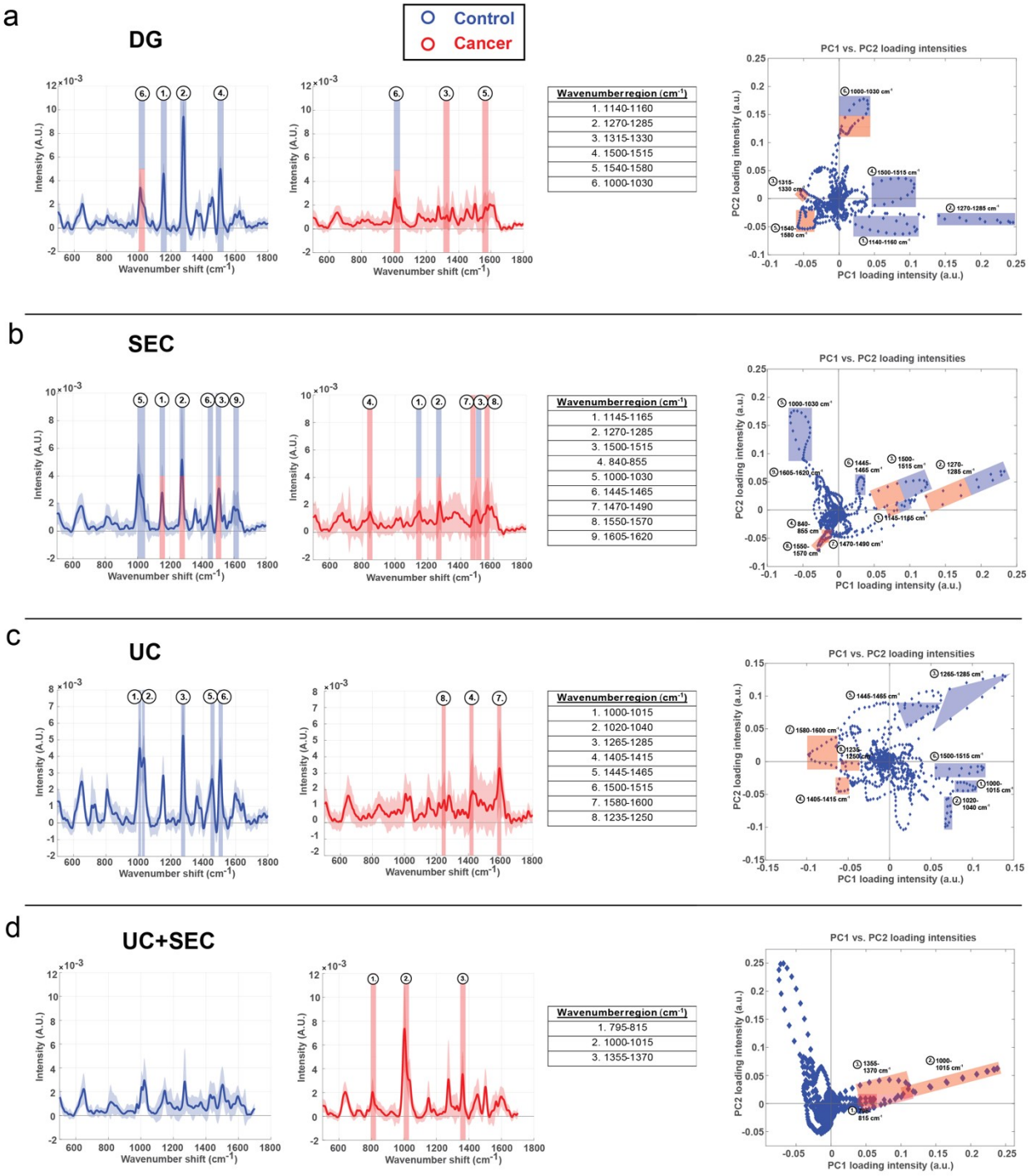


**Supplementary Figure 2: Mean and standard deviation of SERS spectra for EVs isolated from clinical samples.** Spectral features for EVs isolated by either **(a)** DG, **(b)** SEC, **(c)** UC, **(d)** UC-SEC. Blue color denotes EVs isolated from non-cancerous control patients and red represents EVs from head and neck cancer patients. The prominent spectral regions identified by the PCA are color-coded by showing blue/red color for unique or blue-red for shared spectral features across cancer and non-cancer samples. As a visual guide, the PC1 versus PC2 loading intensities are displayed on the right-hand side of each panel. Influential spectral areas are annotated with 1-9 for each isolation method using outward-extending loops for ease of matching to the loadings. Peaks/bands providing negligible separation information are excluded.

**Supplementary References**


1. Sivashanmugan, K. *et al.* Bimetallic nanoplasmonic gap-mode SERS substrate for lung normal and cancer-derived exosomes detection. *J. Taiwan Inst. Chem. Eng.* **80**, 149–155 (2017).
2. Willets, K. A. Surface-enhanced Raman scattering (SERS) for probing internal cellular structure and dynamics. *Analytical and Bioanalytical Chemistry* **394**, 85–94 (2009).
3. Smith, Z. J. *et al.* Single exosome study reveals subpopulations distributed among cell lines with variability related to membrane content. *J. Extracell. Vesicles* **4**, (2015).
4. Witkowska, E., Korsak, D., Kowalska, A., Janeczek, A. & Kamińska, A. Strain-level typing and identification of bacteria – a novel approach for SERS active plasmonic nanostructures. *Anal. Bioanal. Chem.* **410**, 5019–5031 (2018).
5. Mert, S., Özbek, E., Ötünçtemur, A. & Çulha, M. Kidney tumor staging using surface-enhanced Raman scattering. *J. Biomed. Opt.* **20**, 047002 (2015).
6. Chan, J. W., Motton, D., Rutledge, J. C., Keim, N. L. & Huser, T. Raman spectroscopic analysis of biochemical changes in individual triglyceride-rich lipoproteins in the pre- and postprandial state. *Anal. Chem.* **77**, 5870–5876 (2005).
7. Stremersch, S. *et al.* Identification of individual exosome-like vesicles by surface enhanced raman spectroscopy. *Small* **12**, 3292–3301 (2016).
8. Lajos, G., Jancura, D., Miskovsky, P., García-Ramos, J. V. & Sanchez-Cortes, S. Interaction of the photosensitizer hypericin with low-density lipoproteins and phosphatidylcholine: A Surface-enhanced Raman scattering and Surface-enhanced fluorescence study. *J. Phys. Chem. C* **113**, 7147–7154 (2009).
9. Park, J. *et al.* Exosome classification by pattern analysis of surface-enhanced Raman spectroscopy data for lung cancer diagnosis. *Anal. Chem.* **89**, 6695–6701 (2017).
10. Lee, W. *et al.* Label-free prostate cancer detection by characterization of extracellular vesicles using Raman spectroscopy. *Anal. Chem.* **90**, 11290–11296 (2018).
11. Shin, H., Jeong, H., Park, J., Hong, S. & Choi, Y. Correlation between cancerous exosomes and protein markers based on surface-enhanced Raman spectroscopy (SERS) and Principal Component Analysis (PCA). *ACS Sensors* **3**, 2637–2643 (2018).